ISSN 1070-3284, Russian Journal of Coordination Chemistry, 2017, Vol. 43, No. 12, pp. 864–873. © Pleiades Publishing, Ltd., 2017.
Original Russian Text © N.V. Somov, F.F. Chausov, R.M. Zakirova, I.V. Fedotova, N.V. Lomova, I.N. Shabanova, V.G. Petrov, M.A. Shumilova, D.K. Zhirov, 2017, published in Koordinatsionnaya Khimiya, 2017, Vol. 43, No. 12, pp. 765–774.

The Trisodium Monohydrogen-Nitrilo-Tris-Methylenephosphonato-Hydroxylaminato-Nitrosyl-Molybdate Octahydrate $Na_3[Mo(NO)(NH_2O)\{N(CH_2PO_3)_3H\}] \cdot 8H_2O$: Synthesis, Structure, and Nature of Coordination Bond of Transition Metal with Non-Innocent Ligand

N. V. Somov[a, *], F. F. Chausov[b, c], R. M. Zakirova[b], I. V. Fedotova[b], N. V. Lomova[b, c], I. N. Shabanova[c], V. G. Petrov[d], M. A. Shumilova[d], and D. K. Zhirov[d]

[a] *Lobachevsky State University of Nizhny Novgorod, Nizhny Novgorod, 603950 Russia*
[b] *Udmurt State University, Izhevsk, Udmurtiya, 426034 Russia*
[c] *Physical-Technical Institute, Ural Branch, Russian Academy of Sciences, Izhevsk, 426000 Russia*
[d] *Institute of Mechanics, Ural Branch, Russian Academy of Sciences, Izhevsk, 426067 Russia*
**e-mail: xps@ftiudm.ru*

Received June 22, 2017

Abstract—The sodium salt of heteroleptic molybdenum complex with nitrilotris(methylenephosphonic) acid (NTP), hydroxylamine, and nitrogen(II) oxide $Na_3[Mo(NO)(NH_2O)\{N(CH_2PO_3)_3H\}] \cdot 8H_2O$ was synthesized, isolated, and studied (space group $P2_1/c$, $Z = 4$, $a = 9.7385(2)$, $b = 10.2542(2)$, $c = 21.6517(3)$ Å, $\beta = 93.7060(10)°$). The nitrilotris(methylenephosphonate) ion is monoprotonated at the PO_3 group. The nitrogen atom is deprotonated and coordinates the Mo atom; the NTP denticity is 4. Hydroxylamine is ionized according to the acid type and is bidentate. The Mo–NO group is almost linear (176.31(19)° angle; Mo–N, 1.7599(13) Å; ν(N–O), 1756 cm^{-1}), the electron density distribution attests to the formation of an Mo–N π-bond. The Mo coordination polyhedron is a distorted pentagonal bipyramid. Two Na ions are coordinated at the vertices of a distorted octahedron and the third one forms a distorted tetrahedral geometry. (CIF file CCDC no. 1543700.)

Keywords: nitrilotris(methylenephosphonic) acid, molybdenum(III), nitrosyl, hydroxylamine, non-innocent ligand, heteroleptic complex, chelate complex

DOI: 10.1134/S1070328417120090

INTRODUCTION

The abundance and uniqueness of the coordination chemistry of molybdenum, a typical 4*d*-element, are caused by differences from the corresponding 3*d* elements, on the one hand, and from Period 6 *d*-elements, which have the occupied $4f^{14}$-level, on the other hand. Numerous coordination compounds containing Mo in all oxidation states from 0 to +6 are known [1, 2]. The variable oxidation state accounts for the catalytic activity of Mo complexes, including catalysis of functionalization of N_2 and O_2 molecules [3, 4], biological activity as cofactors of many enzymes [5], chiral catalytic activity of oxo, peroxo, imino, and hydrazido complexes [6, 7]. The ability of Mo to form soplisticated clusters accounts for the abundance of the molybdenum supramolecular chemistry [8].

A peculiar redox behavior is inherent in complexes containing so-called non-innocent ligands, that is, ligands (e.g., NO) capable of considerable electron density redistribution with the coordination center with retention of the chemical structure [9, 10]. The redox processes involving complexes with non-innocent ligands can be accompanied by a change in the electron density on either the metal atom or the non-innocent ligand, or both [11–13]. In the cited publications, the redox behavior of complexes with non-innocent ligands has been studied by voltammetry, ESR, and optical spectroscopy, and by numerical electronic structure calculations. The Rh(III), Ir(III), Cu(I), and Hg(II) complexes with nitrosoarenes have been studied by X-ray photoelectron spectroscopy (XPS) [14]. It is pertinent to further investigate the electronic structure and the nature of the coordination bond in transition metal complexes with non-innocent ligands.

Among the N,O-ligands capable of various coordination modes, considerable attention is paid to nitrilo-

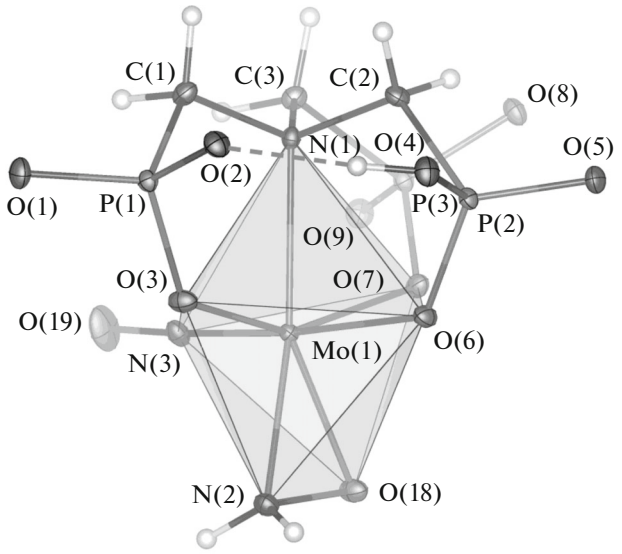

Fig. 1. Structure of the complex anion $[Mo(NO)(NH_2O)\{N(CH_2PO_3)_3H\}]^{3-}$.

tris(methylenephosphonic) acid $N(CH_2PO_3)_3H_6$ (NTP) and its complexes [15, 16]. The NTP complexes of transition metals behave as corrosion inhibitors [17, 18] and bactericides [19, 20]. The stepwise deprotonation of the NTP donor groups over broad pH range gives rise to diverse binding modes of NTP with transition metals. The M–N coordination bond with 3*d*-elements (Co–Zn) is formed, most often, in an alkaline medium after complete deprotonation of all donor centers of the ligand, including the tertiary nitrogen atom [17, 20–22]. However, NTP complexes of molybdenum have not been studied before.

This communication describes the synthesis and structure of the sodium salt of the heteroleptic molybdenum complex with NTP, hydroxylamine, and nitrogen(II) oxide, $Na_3[Mo(NO)(NH_2O)\{N(CH_2PO_3)_3H\}] \cdot 8H_2O$ (**I**).

EXPERIMENTAL

Synthesis of I. Analytical grade hydroxylamine hydrochloride (1.39 g, 0.02 mol) and doubly recrystallized NTP (3.00 g, 0.01 mol) were added to an aqueous solution of reagent grade ammonium paramolybdate (1.77 g, 0.01 mol of Mo(VI)). The reaction mixture was heated for 2 h with continuous stirring, reagent grade sodium hydroxide (2.00 g, 0.05 mol) was added, and the mixture was boiled until the ammonia odor disappeared:

$$(NH_4)_6Mo_7^{VI}O_{24} + 14NH_2OH \cdot HCl + 7N(CH_2PO_3)_3H_6 + 35NaOH = 7Na_3[Mo^{III}(NO)(NH_2O)\{N(CH_2PO_3)_3H\}] + 59H_2O + 14NaCl + 6NH_3\uparrow.$$

The resulting yellow solution (pH 7.4) was filtered. Slow solvent evaporation at room temperature gave crystals of **I** as yellow transparent prisms. The product was washed with ethanol and diethyl ether, and dried in air.

X-ray diffraction. The crystallographic characteristics and X-ray diffraction experiment and structure refinement details for structure **I** are summarized in Table 1. The primary structural fragment was found by the direct method and positions of all atoms, including hydrogens, were found from the difference electron density maps. The non-hydrogen atom parameters were refined in the anisotropic approximation by least squares method on $|F|^2$. The hydrogen atom parameters were refined in the isotropic approximation in the common least squares cycle.

The X-ray diffraction data for **I** are deposited with the crystallographic data centre (CCDC no. 1543700; deposit@ccdc.cam.ac.uk or http://www.ccdc.cam.ac.uk/data_request/cif).

The XPS data for a finely dispersed powder of **I** on an Au substrate (99.9%) were collected on a domestic RES-3 X-ray photoelectron spectrometer (Physical-Technical Institute, Ural Branch, Russian Academy of Sciences) [27] with a magnetic energy analyzer upon excitation with AlK_α radiation ($h\nu$ = 1486.6 eV). The energy analyzer was calibrated against the C1*s* spectrum (binding energy E_B = 285 eV). The background and inelastic scattering corrections were applied according to Shirley [28].

The UV/Vis spectra of aqueous solutions of **I** with concentrations of 5, 1, 0.3, 0.05, and 0.01% were measured with an SF-56 spectrometer in the 190–1100 nm range.

The IR spectra of **I** and the products of its thermal decomposition were recorded for KBr pellets (1 mg sample, 250 mg KBr) on a FSM-1201 FT IR spectrometer in the 450–5000 cm^{-1} range.

The Raman spectrum of a single crystal of **I** was obtained on a Centaur U-HR microscope spectrometer in the 473–573 nm range (λ_{excit} = 473 nm).

Thermogravimetric analysis of **I** was carried out on a Shimadzu DTG-60H automatic differential thermal analyzer in the 30–500°C temperature range and 3°C/min heating rate under argon.

RESULTS AND DISCUSSION

The structure of the complex anion $[Mo(NO)(NH_2O)\{N(CH_2PO_3)_3H\}]^{3-}$ of compound **I** is presented in Fig. 1. The interatomic distances and bond angles are summarized in Table 2.

The complex anion is asymmetric and is described by C_1 point group. The Mo atom is coordinated by seven donor centers: three N atoms and four O atoms of one NTP molecule, one hydroxylamine molecule, and one NO molecule.

Table 1. Crystallographic characteristics and X-ray experiment and structure refinement details for structure **I**

Parameter	Value
Molecular formula	$C_3H_{25}N_3O_{19}P_3Na_3Mo$
M	665.08
System	Monoclinic
Space group; Z	$P2_1/c$; 4
a, Å	9.7385(2)
b, Å	10.2542(2)
c, Å	21.6517(3)
β, deg	93.7060(10)
V, Å^3	2157.63(7)
ρ(calcd.), g/cm ^{3}	2.047
Radiation; λ, Å	MoK_α; 0.71073
μ, mm $^{-1}$	0.983
T, K	293(2)
Crystal size, mm	0.106 × 0.096 × 0.049
Diffractometer	Xcalibur, Sapphire III, Gemini S
Scan mode	ω
Absorption corrections, T_{min}/T_{max}	Empirical [23], 0.85393/1.0
$\theta_{min}/\theta_{max}$, deg	3.755/34.967
Ranges of indexes h, k, l	$-13 \le h \le 13$, $-14 \le k \le 14$, $-30 \le l \le 30$
Number of reflections: measured/unique (N_1)/R_{Int}/with $I > 2\sigma(I)$ (N_2)	44025/6578/0.038/6095
Refinement method	Full-matrix least-squares on F^2
Number of parameters/constraints	385/2
S	1.114
R_1/wR_1 for N_1	0.0294/0.059
R_1/wR_1 for N_2	0.0253/0.0575
$\Delta\rho_{min}/\Delta\rho_{max}$, e/Å^3	−0.52/0.651
Programs	CrysAlisPro [23], SHELX-2014 [24], WinGX [25], VESTA 3.0 [26]

The NTP molecule is monoprotonated at one phosphonate group; the tertiary N atom is deprotonated. In each PO_3 group, one oxygen atom coordinates the Mo atom. In addition, the O(4) and O(9) atoms coordinate the symmetrically equivalent Na(3) atoms, and O(5) coordinates two symmetrically equivalent Na(1) atoms. The other oxygen atoms are involved in hydrogen bonds. The P–O distances considerably depend on the local environment of oxygens: for the O atoms coordinated to Mo, the P–O distances are 1.5289(12)–1.5499(12) Å (average 1.542(9) Å), for the protonated O atom, the P(2)–O(4) distance is 1.5726(13) Å, and for other O atoms, the P–O distances are 1.4952(12)–1.5292(12) Å (average 1.515(12) Å). The coordination to Na atoms does not affect considerably the P–O distances.

The bond angles at the N atom (average 109.5(15)°) corresponds to an ideal tetrahedral angle, which attests to the participation of the nitrogen lone pair in the coordination with Mo. The bond angles at the phosphorus atoms (average 109.4(155)°) also correspond to the tetrahedral angle; however, their large root-mean-square deviations attest to a considerable strain in the PO_3 groups upon chelate ring closure.

The Mo coordination to the NTP molecule is accompanied by closure of three five-membered Mo–N–C–P–O chelate ring sharing the Mo–N bond. With allowance for the hydrogen bond, there is also an eight-membered ring, Mo(1)–O(6)–P(2)–O(4)–H(25)···O(2)–P(1)–O(3). All three Mo–N–C–P–O rings have different conformations: the Mo–O–P–C torsion angles for P(1), P(2), and P(3) are 8.90(5)°, 7.79(3)°, and 22.14(3)°, respectively. The conforma-

Table 2. Interatomic distances (*d*) and bond angles (ω) in structure **I**

Bond	*d*, Å	Bond	*d*, Å	Bond	*d*, Å
Mo(1)–N(1)	2.2771(14)	C(1)–P(1)	1.8128(17)	P(2)–O(5)	1.4952(12)
Mo(1)–N(2)	2.0907(15)	C(2)–P(2)	1.8277(17)	P(2)–O(6)	1.5289(12)
Mo(1)–N(3)	1.7598(14)	C(3)–P(3)	1.8284(17)	P(3)–O(7)	1.5499(12)
Mo(1)–O(3)	2.0968(12)	P(1)–O(1)	1.5167(12)	P(3)–O(8)	1.5292(12)
Mo(1)–O(6)	2.1566(11)	P(1)–O(2)	1.5226(12)	P(3)–O(9)	1.5119(12)
Mo(1)–O(7)	2.0687(11)	P(1)–O(3)	1.5480(12)	N(2)–O(18)	1.3969(18)
Mo(1)–O(18)	2.0332(12)	P(2)–O(4)	1.5726(13)	N(3)–O(19)	1.2121(19)
Na(1)–O	2.3922(14)–2.5161(15)	Na(2)–O	2.3231(16)–2.5556(16)	Na(3)–O	2.3083(14)–2.7443(15)
Na(1)–Na(1)	3.3781(14)	Na(2)–Na(2)	3.6786(14)		
Angle	ω, deg	Angle	ω, deg	Angle	ω, deg
O(6)Mo(1)N(1)	83.33(8)	N(3)Mo(1)N(2)	94.30(10)	O(7)Mo(1)O(18)	80.96(8)
O(6)Mo(1)O(3)	83.76(7)	N(3)Mo(1)O(18)	97.50(9)	*a**–Mo(1)–*b**	67.45(10)
O(6)Mo(1)O(7)	82.52(8)	N(3)Mo(1)O(6)	175.00(11)	*a**–Mo(1)O(3)	70.26(10)
O(6)Mo(1)N(2)	90.57(9)	N(1)Mo(1)O(3)	78.90(8)	*b**–Mo(1)O(7)	66.85(10)
O(6)Mo(1)O(18)	86.96(9)	N(1)Mo(1)O(7)	75.23(8)	Mo(1)N(3)O(19)	176.31(19)
N(3)Mo(1)N(1)	91.68(10)	N(2)Mo(1)O(3)	84.01(9)	Mo(1)N(2)O(18)	68.00(12)
N(3)Mo(1)O(3)	95.64(10)	N(2)Mo(1)O(18)	39.57(8)	Mo(1)O(18)N(2)	72.44(12)
N(3)Mo(1)O(7)	95.91(9)				
ONa(1)O	163.15(9)–176.26(10); 78.60(8)–95.66(8)	ONa(2)O	165.46(10)–179.12(9); 82.42(8)–97.54(9)	ONa(3)O	93.66(9)–134.67(10)

* The electron density maxima *a* and *b* are shown in Fig. 3a.

tion of the NTP ligand in **I** is close to that observed in the Ni complex [21].

The hydroxylamine molecule in complex **I** is singly ionized according to acid type and is N,O-coordinated to Mo. Such a coordination of hydroxylamine is encountered only in the complexes of some transition metals (Mo, V, U) [29–31].

The NO radical molecule is coordinated to Mo via nitrogen. The Mo(1)–N(3) distance of 1.7598(14) Å is considerably shorter than the sum of the Mo and N covalent radii for a single bond (r_1(Mo) = 1.54(5) Å [32]; 1.38 Å [33]; r_1(N) = 0.71(1) Å [32, 33]). The observed Mo(1)–N(3) distance is intermediate between the sums of the covalent radii for the double bond [34] (r_2(Mo) = 1.21 Å; r_2(N) = 0.60 Å) and the triple bond [35] (r_3(Mo) = 1.13 Å; r_3(N) = 0.54 Å). This indicates that the Mo(1)–N(3) bond is multiple. The N(3)–O(19) distance (1.2121(19) Å) is closer to the sum of the covalent radii for the double bond [34] (r_2(O) = 0.57 Å) than for the single bond (r_1(O) = 0.66(2) Å [32]; 0.63 Å [33]).

An unusual acid-base behavior of N,O-ligands is observed: the relatively basic tertiary nitrogen atoms of NTP (pK = 12.9(1) [36]) and oxygen atoms of hydroxylamine (pK = 13.7 [37]) are deprotonated, whereas more acidic (pK = 7.22(3) [38]) PO_3H group is retained.

The crystal packing of **I** is presented in Fig. 2. The packing is 2D-layered (Fig. 2a): the (001) and (002) planes are formed by layers composed of 1D-chains of Na(1) and Na(2) coordination polyhedra (CP), which run along the [$2\bar{2}0$] axes in the (001) plane (Fig. 2b) and along the [220] axes in the (002) plane. Two adjacent vertices of the Na(1) CP are occupied by the O(5) atoms of two NTP molecules symmetrically equivalent relative to the inversion center; the inversion center is located in the midpoint of the octahedron edge connecting the O(5) atoms and common to the two symmetrically equivalent Na(1) polyhedra. The other Na(1) CP vertices are occupied by H_2O molecules. Two of these molecules are bridging and bind the Na(1) and N(2) CP by the shared O(11)–O(12) edge. All vertices of Na(2) CP are occupied by H_2O molecules. The neighboring Na(2) coordination polyhedra are connected to one another by a shared O(15)–O(15) edge in the midpoint of which the inversion center is located. The 2_1 axes around which the complex anions are arranged occur in the (004) planes (Fig. 2c). The Na(3) CP is linked to the Na(1) CP by one vertex (occupied by the O(17) water molecule);

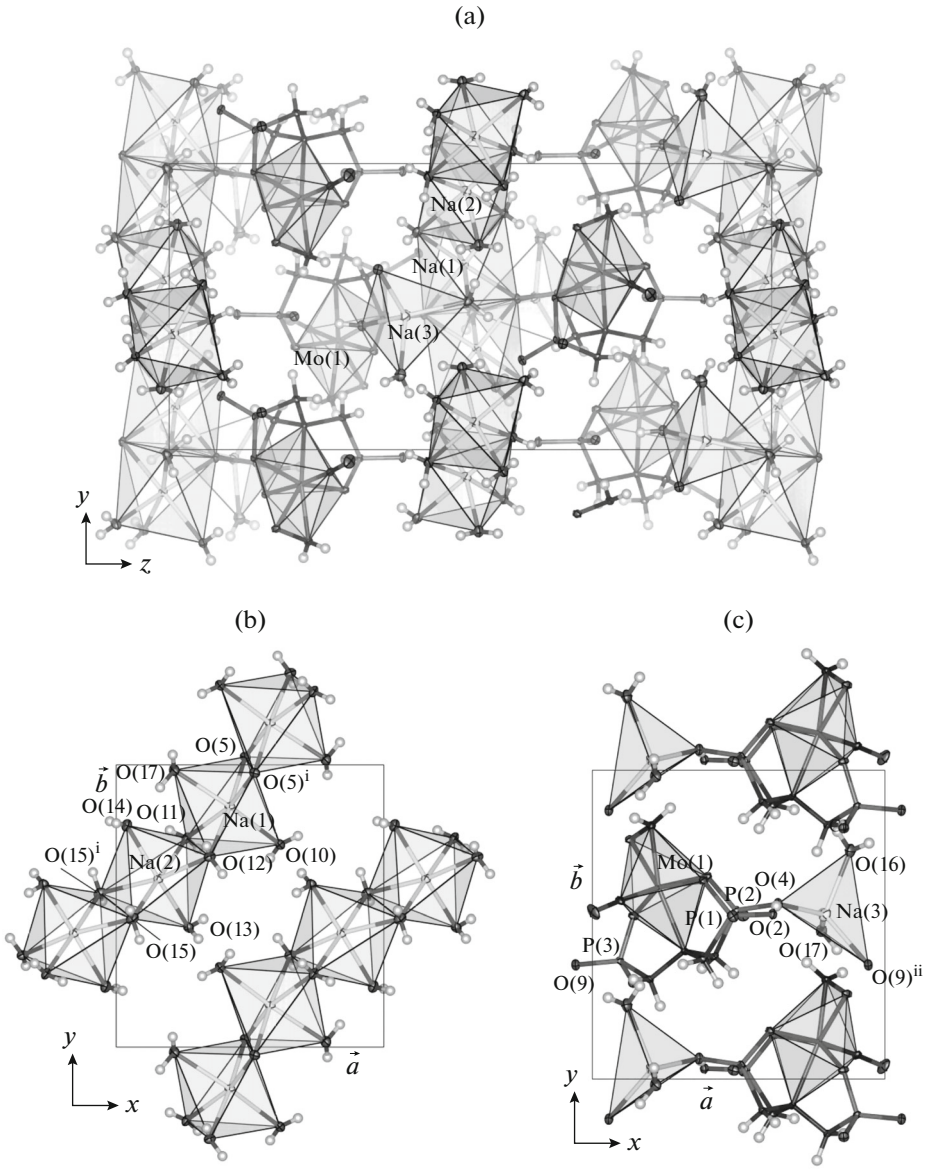

Fig. 2. Crystal packing of **I**: (a) layers of complex anions and hydrated Na^+ ions (projection onto the (100) plane); (b) layer of hydrated Na^+ ions in the (001) plane; (c) layer of complex anions in the (004) plane; symmetry codes: [i] $-x, -y, -z$; [ii] $x + 1, y, z$.

the other two vertices are occupied by the O(4) and O(9) atoms of two NTP molecules symmetrically equivalent relative to the *a* translation. The fourth vertex of the Na(3) CP accommodates the H_2O molecule. Apart from coordination bonds, the layers of the crystal packing are connected by the Coulomb attraction forces and hydrogen bonds (Table 3).

The geometric configuration of the metal CP was estimated by calculating the similarity coefficient ($\Phi(T, S)$) for the experimentally determined polyhedron *T* and reference polyhedron *S* by a previously described method [39]. The calculations were carried out by the Polyhedron program from the PseudoSymmetry program package (http://phys.unn.ru/ps) with the sensitivity parameter $\lambda = 1.1914$ rad^{-1}. The Mo atom coordination geometry is a distorted (Φ = 0.1310(1)) pentagonal bipyramid (C.N. 7), with the N(3) atom of the NO radical molecule and the O(6) atom of the NTP molecule being in the axial vertices. The Na(1) and Na(2) atoms are coordinated according to a distorted octahedral geometry (C.N. 6) (Φ = 0.3626(1) and 0.3555(1), respectively). The Na(3) atom forms a distorted tetrahedron (C.N. 4) (Φ = 0.4411(8)).

The molecular vibrational spectra of **I** (Fig. 3) confirm the described structure. According to published data [40] and the reported correlation between the characteristic ν(Mo–O) frequencies and the Mo–O

Table 3. Geometric parameters of hydrogen bonds in the crystal packing of **I**

D–H···A	Distance, Å			D–H···A angle, deg
	D–H	H···A	D···A	
O(4)–H(25)···O(2)	0.82(3)	1.66(3)	2.4711(17)	175(3)
O(17)–H(24)···O(14)^{i}	0.851(2)	1.845(6)	2.6860(19)	170(3)
O(13)–H(14)···O(1)^{ii}	0.74(3)	1.95(3)	2.6942(18)	175(3)
O(14)–H(21)···O(8)^{iii}	0.87(3)	1.84(3)	2.7050(18)	171(3)
O(16)–H(7)···O(18)	0.85(3)	1.91(3)	2.7054(19)	156(3)
O(16)–H(8)···O(13)^{iv}	0.83(3)	1.90(3)	2.713(2)	169(3)
O(11)–H(12)···O(9)	0.74(3)	2.00(3)	2.7245(18)	169(3)
O(13)–H(13)···O(10)^{v}	0.79(3)	1.95(3)	2.7325(19)	177(3)
O(10)–H(10)···O(1)^{vi}	0.77(3)	1.98(3)	2.7435(18)	172(3)
O(14)–H(22)···O(16)^{iii}	0.81(3)	2.01(3)	2.791(2)	164(3)
O(10)–H(9)···O(8)	0.80(3)	2.02(3)	2.8220(18)	174(3)
O(12)–H(20)···O(6)	0.68(3)	2.22(3)	2.8633(18)	156(3)
O(12)–H(19)···O(1)^{vii}	0.82(3)	2.05(3)	2.8660(19)	173(3)
O(15)–H(17)···O(8)^{viii}	0.81(3)	2.06(3)	2.868(2)	173(3)
N(2)–H(16)···O(2)^{ix}	0.90(2)	2.00(2)	2.8809(19)	167(2)
O(15)–H(18)···O(19)^{viii}	0.75(3)	2.28(3)	2.950(2)	149(3)
N(2)–H(15)···O(9)^{ix}	0.87(2)	2.15(2)	2.9832(19)	161(2)
O(17)–H(23)···O(8)^{i}	0.90(2)	2.12(2)	2.9899(18)	161(3)
O(11)–H(11)···O(3)^{ii}	0.81(3)	2.32(3)	3.0957(18)	161(3)

Symmetry codes: ^{i} $-x, -y+1, -z+1$; ^{ii} $x, -y+1/2, z-1/2$; ^{iii} $x-1, y, z$; ^{iv} $x-1, y-1, z$; ^{v} $-x+1, -y, -z+1$; ^{vi} $x, -y+1/2, z+1/2$; ^{vii} $-x+1, y+1/2, -z+1/2$; ^{viii} $x, y-1, z$; ^{ix} $-x, y1/2 -z+1/2$.

distance [41], the internal Mo–O bond vibrations correspond to the following bands (cm^{-1}): 179, 220, 270, 310 δ(O–Mo–O), 374 ν(Mo(1)–O(6)), 468 ν(Mo(1)–O(3)/O(7)), 506 ν(Mo(1)–O(18)). The band at 563 cm^{-1}, which is absent from the Raman spectra, corresponds apparently to the Mo(1)–N(3) stretching modes [42]. The bending vibrations of the NTP molecule are responsible for the following bands (cm^{-1}): 600–673 δ(O–P–O), 820–895 δ(N–C–P). The asymmetric configuration of the NTP molecule is manifested if these bands are not forbidden. The 922 cm^{-1} band, which is inactive in the Raman spectra, refers to the N(2)–O(18) stretching modes of the hydroxylamine molecule [43, 44]. The ν(P–O) modes are manifested at 970, 985, 1043, 1080, 1112, 1179, and 1198 cm^{-1}. The isolated P–O π-bonds give rise to a strong broad band at 1235–1320 cm^{-1} in the Raman spectrum and to three weak bands at 1239, 1270, and 1300 cm^{-1} in the IR spectrum, which confirms the non-equivalence of three PO_3 groups. The 1325, 1340, 1355, and 1381 cm^{-1} bands are attributable to the δ(Na–O–H) vibrations. The broad IR band at 1410–1464 cm^{-1} corresponds to three δ_s–$\delta_{as}(CH_2)$ doublets of the symmetrically non-equivalent branches of the NTP molecule. In the Raman spectrum, the CH_2 vibrations are responsible for only an asymmetric mode at about 1445 cm^{-1}. The broad asymmetric band at 1490–1580 cm^{-1} observed only in the IR spectrum can be assigned to the δ_s–$\delta_{as}(H_2O)$ vibrations in the CP of Na^+ ions. The doublet at 1630–1677 cm^{-1} corresponds to the δ_s–$\delta_{as}(NH_2)$ vibrations of the hydroxylamine molecule. The nitroso group vibrations ν(N–O) are manifested at 1756 cm^{-1}, which is consistent with published data for linear nitroso group [42]. The following bands are also observed (cm^{-1}): 2873 ν(OH), 2950 ν(CH_2), 3185, 3220 ν(NH_2), 3320, 3390, 3444, 3500, and 3538 ν(H_2O).

In the UV/Vis spectra of aqueous solutions of **I** (Fig. 4), it is possible to distinguish charge transfer bands with peaks at 220, 238, and 248 nm and *d*–*d*-transition bands with peaks at 298 and 343 nm. The observed UV/Vis spectrum corresponds to that of an aqueous solution of the $K_4Mo(CN)_7$ complex containing a pentagonal-bipyramidal Mo^{3+} ion [45].

The XPS spectrum of **I** is shown in Fig. 5. The P2*p* line has one component with E_B = 131.5 eV and full width at half maximum (FWHM) of 2.3 eV, which

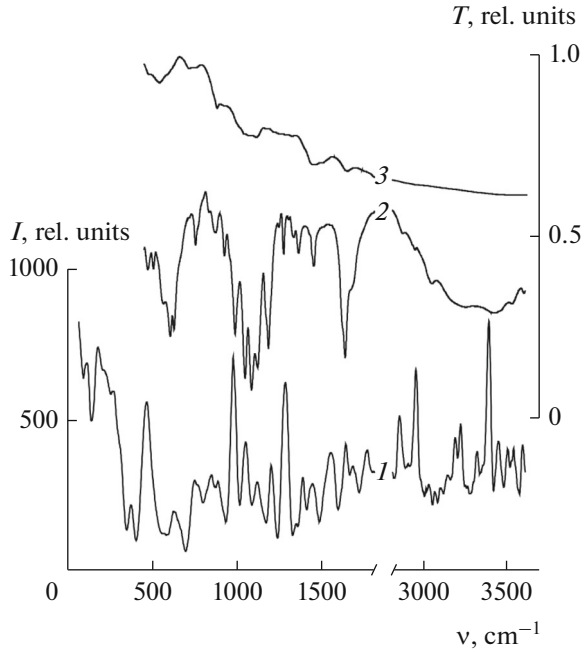

Fig. 3. (*1*) Raman spectrum of a single crystal of **I**; IR spectra of (*2*) **I** and (*3*) the products of thermal decomposition of **I** under argon.

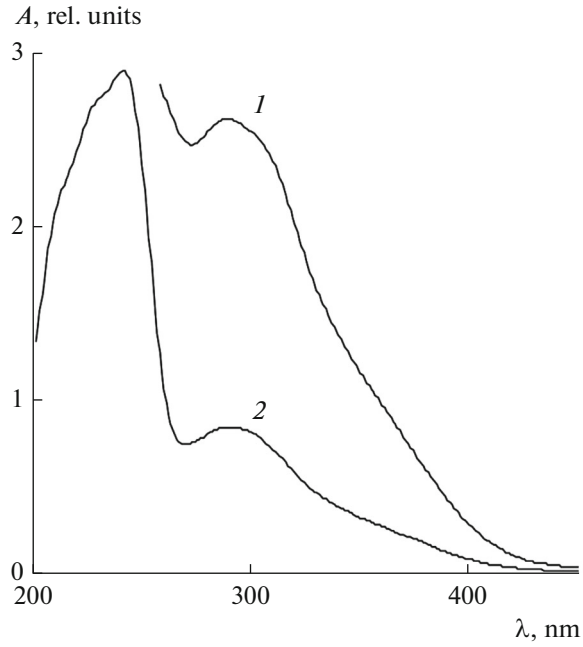

Fig. 4. UV/Vis spectra of aqueous solutions of **I** with concentrations: (*1*) 1 and (*2*) 0.3%.

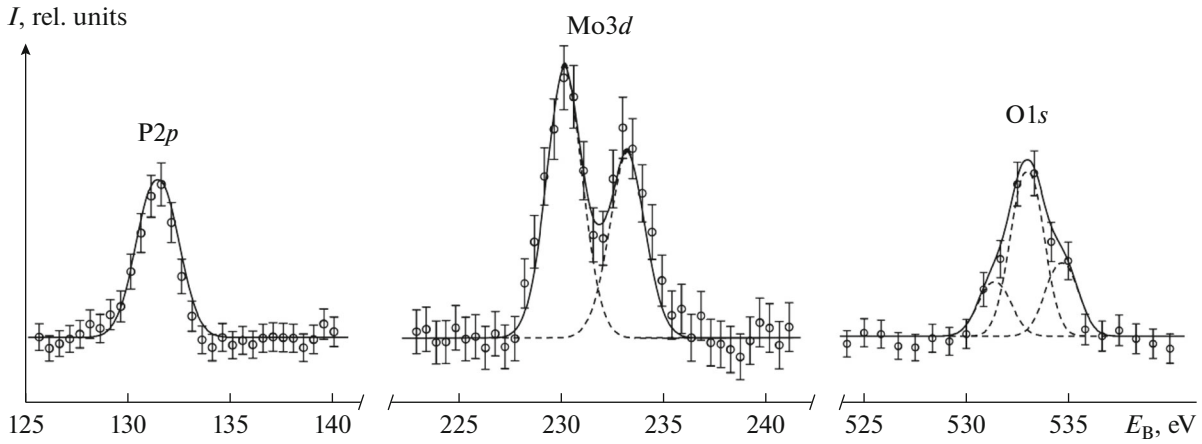

Fig. 5. X-ray photoelectron spectrum of **I**.

attests to insignificant differences in the local environments of three phosphorus atoms.

For the Mo3$d_{5/2-3/2}$ spin–orbit doublet, E_B = 230.1 and 233.2 eV, FWHM = 2.2 eV. The extensive literature data indicate that the binding energies of the Mo3$d_{5/2-3/2}$ doublet components cannot serve as evidence for the formal oxidation state of molybdenum; indeed, E_B = 229.4–230.8 for the Mo3$d_{5/2}$ line and E_B = 232.6–233.8 for the Mo3$d_{3/2}$ line are typical of both Mo^{3+} and Mo^{4+} complexes [46]. However, there is close correlation between the binding energies of the Mo3$d_{5/2-3/2}$ doublet components and the effective charge of the molybdenum ion [47, 48]. According to [47], E_B = 233.2 eV for the Mo3$d_{3/2}$ line is close to that for the $[MoCl_2(NO)_2\{P(C_6H_5)_3\}_2]$ complex in which the effective charge of the Mo atom, q_{Mo} = 0.8e (e = 1.60 × 10^{-19} C). According to [48], the position of the Mo3$d_{5/2}$ line is close to the data for $MoCl_5$ where q_{Mo} = 0.9e. Thus, the Mo effective charge in **I** can be estimated as 0.8–0.9 e.

The O1*s* line has a complex profile and can be represented as a superposition of three components with

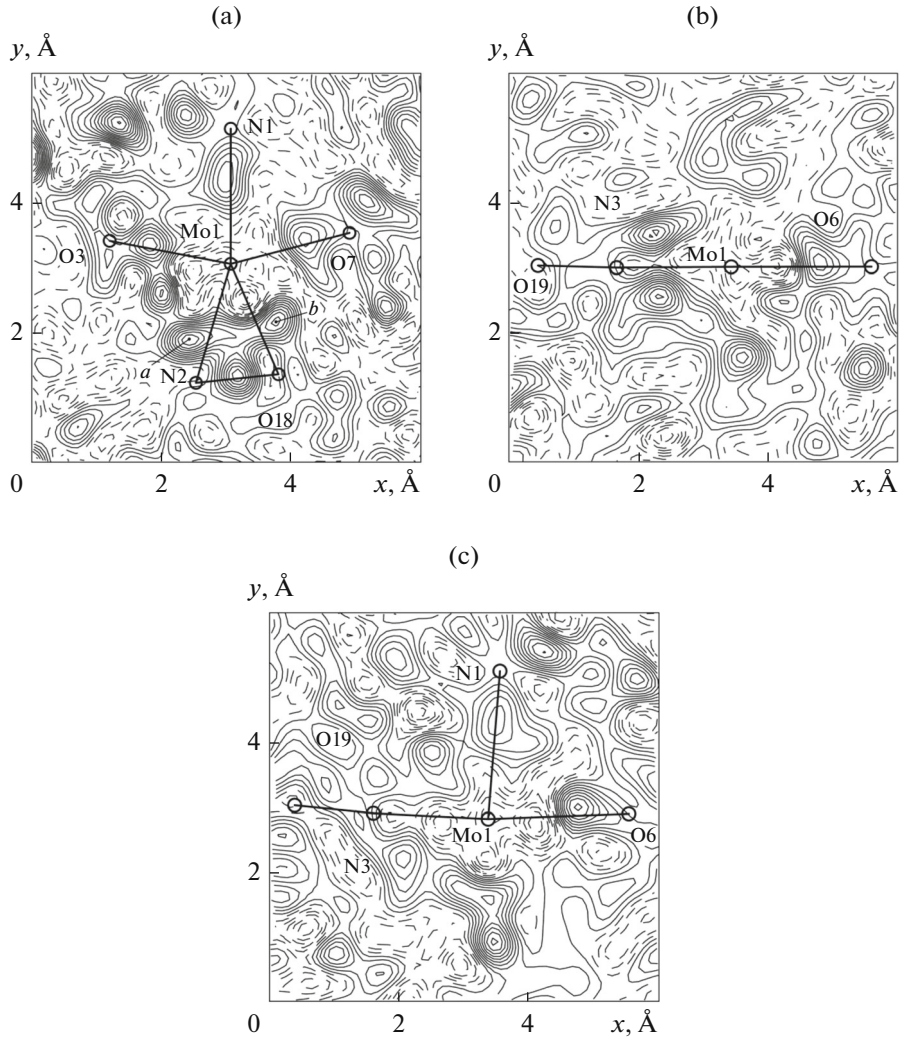

Fig. 6. Difference electron density maps $\rho_{exp}-\rho_{calc}$ in the planes: (a) $(31\bar{6})$; (b) $(1\bar{3}0)$; (c) (216). The step of isolines 0.05 $e/Å^3$; excess density isolines are continuous and deficient density isolines are dashed.

E_B = 531.2, 532.9, and 534.6 eV and FWHM = 1.8 eV; the exact assignment of these components is problematic.

The analysis of XPS spectra shows that the effective charge of the Mo atom in **I** is much lower than the formal oxidation state. This can be attributed to the electron density migration from the non-innocent $NO^{\bullet}$ ligand to the Mo atom. For studying the electron density distribution in the inner coordination sphere of **I**, difference electron density maps $\rho_{exp}-\rho_{calc}$ were constructed using X-ray diffraction data in the $(31\bar{6})$, $(1\bar{3}0)$ and (216) crystallographic planes, in which the characteristic fragments of the $[Mo(NO)(NH_2O)\{N(CH_2PO_3)_3H\}]^{3-}$ anion are located (Fig. 6).

In the $(31\bar{6})$ plane (Fig. 6a), Mo has a nearly pentagonal environment composed of the N(1), O(3), and O(7) atoms of the NTP molecule on one side and the N(2) and O(18) atoms of hydroxylamine on the other side. All of the coordination bonds formed by Mo are covalent, as indicated by the excess electron density areas between Mo and each donor center. The bidentate coordination of hydroxylamine gives rise to a highly strained three-membered ring with the O(18)Mo(1)N(2) bond angle of 39.57(8)°. However, because of Coulomb repulsion, the excess electron density clouds *a* and *b* shift away from the lines of the Mo(1)–N(2) and Mo(1)–O(18) bonds and the *a*–Mo(1)–*b* angle (67.45(10)°) is much closer to a regular pentagonal angle. The excess electron density areas *a* and *b* considerably overlap with the electron density of the N(2)–O(18) bond, thus forming a common electronic system of the hydroxylamine molecule and the Mo(1) atom; this implies that the coordination bond formed upon the N,O-coordination of hydroxylamine is partially of the "hapto" nature.

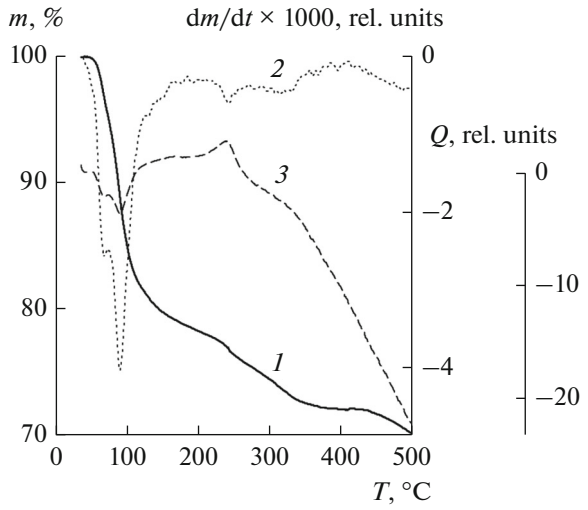

Fig. 7. Thermal analysis curves of **I** in argon. (*1*) Sample mass *m*; (*2*) derivative d*m*/d*t*; and (*3*) thermal effect *Q* as functions of temperature *T*.

In the $(1\bar{3}0)$ plane (Fig. 6b), two intense electron density maxima symmetric relative to the bond line, corresponding to a π-bond, are observed in the Mo(1)–N(3) region. A small electron density maximum occurs between the N(3) and O(19) atoms. Both a deep electron density minimum and an electron density maximum shifted towards O(6) are detected in the Mo(1)–O(6) line, which is attributable to the *trans*-effect of the π-donor NO$^{\cdot}$ ligand. Due to the *trans*-effect, the Mo(1)–O(6) bond is 0.074 Å longer than the average Mo(1)–O(3) and Mo(1)–O(7) bond lengths.

In the (216) plane (Fig. 6c), an area of enhanced electron density inclined with respect to the bond line occurs between the N(3) and O(19) atoms. The same electron density distribution has been calculated for the single-electron N···O molecular orbital [11].

Hence, the coordination of the NO$^{\cdot}$ radical molecule by the Mo atom is accompanied by electron density transfer from the N≡O bond to give a linear system of multiple bonds, Mo≡N=O.

The thermal decomposition of **I** under Ar (Fig. 7) starts with elimination of water molecules in three stages: 45–75°C ($-2H_2O$), 75–125°C ($-5H_2O$), and 125–200°C ($-H_2O$). At 200–270°C, the NH_3 molecule is eliminated; the exothermic effect, attests apparently to opening of the strained ring. Over a broad temperature range of 270–400°C, the mass loss corresponds to the NO molecule. According to published data [49–52], many nitroso complexes of transition metals eliminate NO in the 300–400°C range. In the range of 300–350°C, the shape of the thermal curve sharply changes, probably, due to a phase transition with the change in the sample heat capacity. The IR spectrum of the thermal decomposition products of **I** (Fig. 3, *3*) exhibits broad bands typical of amorphous sodium metaphosphate $NaPO_3$ [53, 54] (cm^{-1}): 470, 540 δ(O–P–O), 1000 ν(PO_3), 1320 ν(P=O) and the molybdenum phosphate glass $MoO_x \cdot P_2O_5$ [55] (cm^{-1}): 760, 853 ν(P–O–P), 1030, 1120, 1260 ν(PO_3), 1650. The incompletely resolved doublet at about 1450 cm^{-1} (probably, δ_s–$\delta_{as}(CH_2)$) indicates that some organic fragments are retained in the molecule at 500°C.

ACKNOWLEDGMENTS

This work was performed in terms of the basic part of the Government Task for higher educational and research institutions in the field of scientific research (project no. 3.6502.2017/BCh).

REFERENCES

1. *Comprehensive Coordination Chemistry*, Wilkinson, G., Gillard, R.D., and McCleverty, J.A., Eds. Pergamon Press, 1987, vol. 3.
2. *Comprehensive Coordination Chemistry II*, McCleverty, J.A. and Meyer, T.J., Eds., Elsevier, 2003, vol. 4.
3. Klopsch, I., Yuzik-Klimova, E.Yu., and Schneider, S., *Nitrogen Fixation: Top. Organomet. Chem.*, 2017, vol. 60, p. 71.
4. Amini, M., Haghdoost, M.M., and Bagherzadeh, M., *Coord. Chem. Rev.*, 2013, vol. 257, p. 1093.
5. Iobbi-Nivol, C. and Leimkuhler, S., *Biochim. Biophys. Acta*, 2013, vol. 1827, p. 1086.
6. Malcolmson, S.J., Meek, S.J., Sattely, E.S., et al., *Nature*, 2008, vol. 456, p. 933.
7. Brito, J.A., Royo, B., and Gómez, M., *Catal. Sci. Technol.*, 2011, vol. 1, p. 1109.
8. Müller, A., Das, S.K., Kögerler, P., et al, *Angew. Chem., Int. Ed. Engl.*, 2000, vol. 39, p. 3413.
9. Jørgensen, C.K., *Coord. Chem. Rev.*, 1966, vol. 1, p. 164.
10. Butin, K.P., Beloglazkina, E.K., and Zyk, N.V., *Russ. Chem. Rev.*, 2005, vol. 74, p. 531.
11. Serres, R.G., Grapperhaus, C.A., Bothe, E., et al., *J. Am. Chem. Soc.*, 2004, vol. 126, p. 5138.
12. McCleverty, J.A. and Ward, M.D., *J. Chem. Sci. (Proc. Indian Acad. Sci.)*, 2002, vol. 114, p. 291.
13. Ward, M.D. and McCleverty, J.A., *Dalton Trans.*, 2002, no. 3, p. 275.
14. Vasapollo, G., Nobile, C.F., Sacco, A., et al., *J. Organomet. Chem.*, 1989, vol. 378, p. 239.
15. Cabeza, A., Ouyang, X., Sharma, C.V.K., et al., *Inorg. Chem.*, 2002, vol. 41, p. 2325.
16. Demadis, K.D., Katarachia, S.D., and Koutmos, M., *Inorg. Chem. Commun.*, 2005, vol. 8, p. 254.
17. Somov, N.V. and Chausov, F.F., *Cryst. Rep.*, 2014, vol. 59, no. 1, p. 66.
18. Shabanova, I.N., Chausov, F.F., Naimushina, E.A., and Somov, N.V., *Surf. Interface Anal.*, 2014, vol. 46, p. 750.

19. Somov, N.V. and Chausov, F.F., *Cryst. Rep.*, 2016, vol. 61, no. 1, p. 39.
20. Somov, N.V. and Chausov, F.F., *Cryst. Rep.*, 2015, vol. 60, no. 2, p. 210.
21. Somov, N.V., Chausov, F.F., Zakirova, R.M., and Fedotova, I.V., *Cryst. Rep.*, 2016, vol. 61, no. 2, p. 216.
22. Somov, N.V., Chausov, F.F., Zakirova, R.M., and Fedotova, I.V., *Russ. J. Coord. Chem.*, 2015, vol. 41, no. 12, p. 798.
23. *CrysAlisPro 1.171.38.4*, Rigaku Oxford Diffraction, 2015.
24. Sheldrick, G.M., *Acta Crystallogr., Sect. A: Found. Crystallogr.*, 2008, vol. 64, p. 112.
25. Farrugia, L.J., *J. Appl. Crystallogr.*, 1999, vol. 32, p. 837.
26. Momma, K. and Izumi, F., *J. Appl. Crystallogr.*, 2011, vol. 44, p. 1272.
27. Trapeznikov, V.A., Shabanova, I.N., Kholzakov, A.V., and Ponomaryov, A.G., *J. Electron Spectrosc. Relat. Phenom.*, 2004, vols. 137–140, p. 383.
28. Shirley, D.A., *Phys. Rev.*, 1972, vol. 55, p. 4709.
29. Wieghardt, K., Hobbach, W., Weiss, J., et al., *Angew. Chem., Int. Ed. Engl.*, 1979, vol. 18, no. 7, p. 548.
30. Nuber, B. and Weiss, J., *Acta Crystallogr., Sect. B: Struct. Crystallogr. Cryst. Chem.*, 1981, vol. 37, p. 947.
31. Van Tets, A. and Adrian, H.W.W., *Acta Crystallogr., Sect. B: Struct. Crystallogr. Cryst. Chem.,* 1977, vol. 33, p. 2997.
32. Cordero, B., Gomez, V., Platero-Prats, A.E., et al., *Dalton Trans.*, 2008, no. 21, p. 2832.
33. Pyykkö, P. and Atsumi, M., *Chem.-Eur. J.*, 2009, vol. 15, p. 186.
34. Pyykkö, P. and Atsumi, M., *Chem.-Eur. J.*, 2009, vol. 15, p. 12770.
35. Pyykkö, P., Riedel, S., and Patzschke, M., *Chem.-Eur. J.*, 2005, vol. 11, p. 3511.
36. Popov, A., Rönkkömäki, H., Popov, K., et al., *Inorg. Chim. Acta*, 2003, vol. 353, p. 1.
37. Hughes, M.N., Nicklin, H.G., and Shrimanker, K., *J. Chem. Soc. A*, 1971, p. 3485.
38. Deluchat, V., Bollinger, J.-C., Serpaud, B., and Caullet, C., *Talanta*, 1997, vol. 44, p. 897.
39. Somov, N.V., Chausov, F.F., and Zakirova, R.M., *Cryst. Rep.*, 2017, vol. 62, no. 5, p. 695.
40. Clark, R.J.H., Hempleman, A.J., and Kurmoo, M., *J. Chem. Soc., Dalton Trans.*, 1988, p. 973.
41. Hardcastle, F.D. and Wachs, I.E., *J. Raman Spectrosc.*, 1990, vol. 21, p. 683.
42. De La Cruz, C. and Sheppard, N., *Spectrochim. Acta, Part A*, 2011, vol. 78, p. 7.
43. Giguère, P.A. and Liu, I.D., *Canadian J. Chem.*, 1952, vol. 30, p. 948.
44. Hughes, M.N. and Shrimanker, K., *Inorg. Chim. Acta*, 1976, vol. 18, p. 69.
45. Rossman, G.R., Tsay, F.-D., and Gray, H.B., *Inorg. Chem.*, 1973, vol. 12, p. 824.
46. Chatt, J., Elson, C.M., Leigh, G.J., and Connor, J.A., *J. Chem. Soc., Dalton Trans.*, 1976, p. 1351.
47. Hughes, W.B. and Baldwin, B.A., *Inorg. Chem.*, 1974, vol. 13, p. 1531.
48. Grim, S. and Matienzo, L.J., *Inorg. Chem.*, 1975, vol. 14, p. 1014.
49. Masuda, H., Miyokawa, K., and Masuda, I., *Thermochim. Acta*, 1985, vol. 84, p. 331.
50. Mohai, B., Horváth, A., and Honti, P.E., *J. Therm. Anal.*, 1986, vol. 31, p. 157.
51. Makhinya, A.N., Korolkov, I.V., Il'in, M.A., et al., *J. Chem. Sci.*, 2017, vol. 129, p. 441.
52. Makhinya, A.N., Il'in, M.A., and Baidina, I.A., et al., *J. Struct. Chem.*, 2014, vol. 55, p. 311.
53. Ogden, J.S. and Williams, S.J., *J. Chem. Phys.*, 1980, vol. 73, no. 4, p. 2007.
54. Bencivenni, L. and Gingerich, K.A., *J. Mol. Struct.*, 1983, vol. 98, p. 195.
55. Hekmat-Shoar, M.K., Hogarth, C.A., and Moridi, G.R., *J. Mater. Sci.*, 1991, vol. 26, p. 904.

Translated by Z. Svitanko